



The adsorption of Ag₃Sn nano-particles on Cu–Sn intermetallic compounds of Sn–3Ag–0.5Cu/Cu during soldering

Xiaoying Liu^a, Mingliang Huang^a, Yanhui Zhao^a, C.M.L. Wu^b, Lai Wang^{a,*}

^a Department of Materials Engineering, Dalian University of Technology, Dalian, Liaoning 116024, China

^b Department of Physics and Materials Science, City University of Hong Kong, Hong Kong, China

ARTICLE INFO

Article history:

Received 5 October 2009

Received in revised form

18 November 2009

Accepted 18 November 2009

Available online 22 November 2009

Keywords:

Sn–3Ag–0.5Cu

Cu₆Sn₅

Ag₃Sn

Intermetallic compound (IMC)

Adsorption

ABSTRACT

The interfacial reactions between Sn–3Ag–0.5Cu solder and Cu substrate at 250 °C and 300 °C from 30 s up to 1800 s were investigated. The average size of the Ag₃Sn nano-particles adsorbed on the Cu₆Sn₅ intermetallic compounds as a function of soldering temperature and time were studied. The results show that the adsorption of Ag₃Sn particles occurs during solidification process and the number of Ag₃Sn particles increases with the morphology changing of Cu₆Sn₅ intermetallic compounds. When soldering at a fixed temperature, the average sizes of the Ag₃Sn nano-particles are almost the same with the different soldering durations. However, the Ag₃Sn nano-particles observed on intermetallic compounds are smaller at 300 °C than those at 250 °C. The Ag₃Sn particles arrange in line in the same plane and the arrangements of Ag₃Sn lines order two perpendicular orientations, but there are no relationship with the Cu₆Sn₅ surface orientations.

© 2009 Elsevier B.V. All rights reserved.

1. Introduction

Currently there is an increasing trend to use lead-free solders in microelectronic devices due to environmental issues [1]. In order to meet the required mechanical properties, adequate wettabilities as well as the comparable melting temperature, eutectic Sn–Ag and Sn–Ag–Cu lead-free solders have been considered to replace lead–tin ones [2–4]. The microstructures of these lead-free solders are different from that of eutectic Sn–Pb. Some dispersion phases, such as Ag₃Sn and Cu₆Sn₅, distribute uniformly in the solder matrix. A survey of the literature showed that three types of Ag₃Sn compounds during solidification at different cooling rates were found to be particle-like, needle-like and plate-like [5]. Different cooling rates and Ag contents resulted in different types of Ag₃Sn. Especially, plate-like Ag₃Sn has been widely studied in recent investigations. The plate-like Ag₃Sn could influence the growth and morphology of Cu₆Sn₅ IMC and the stability of the solder joint [6–8]. Large Ag₃Sn plates could adversely affect the plastic deformation properties of the solder [9] and caused plastic-strain localization at the boundary between the Ag₃Sn plates and the bounding β-Sn phase [10]. In practice, many researchers believed that large Ag₃Sn platelets exhibited a mixture of both ductile and brittle fractures [9,11], while fine Ag₃Sn particles formed in the

solder would strengthen the solder matrix [12,13]. Besides these bulk Ag₃Sn compounds, researchers also found some nano-sized Ag₃Sn particles adsorbed on Sn–Ag–Cu/Cu or Ni interface after soldering and aging. Yu et al. [14] has reported that nano-sized Ag₃Sn particles were present on the surface of IMCs when Ni and Cu substrates were dipped into the molten Sn–3.5Ag–0.7Cu and Sn–3.5Ag solders. The existence of these particles would decrease the interfacial energy and suppress the growth of the IMC layer. Wu and Huang [15] have found that tiny Ag₃Sn particles were embedded in the Ni₃Sn₄ or Cu₆Sn₅ grains during aging. Qi et al. [16] have investigated the different formation mechanisms of Ag₃Sn both in the solder and near the interface under thermal shearing cycling condition. They found that the Ag₃Sn particles formed first on η-Cu₆Sn₅ substrate and the coarsening of Ag₃Sn would inhibit the further growth of Cu₆Sn₅ in thermal cycling. So the shape and distribution of Ag₃Sn phase in the solder joints are critical issues for the reliability of solder joints. However, the formation mechanism and influencing factors for nano-sized Ag₃Sn particles are unclear. According to this issue, the adsorption of Ag₃Sn nano-particles on Cu–Sn IMCs at different soldering temperatures, soldering time and cooling rate are studied in the present work.

2. Experimental procedures

Commercial Sn–3Ag–0.5Cu powders with the size of 30–45 μm were mixed with RMA (Rosin Mildly Active) flux to form solder paste. For the substrate, 99.9% pure polycrystalline Cu with the size of 8 mm × 8 mm × 0.1 mm and single crystal Cu disk of Ø8 mm × 0.1 mm were used. After polishing, the coupons were degreased

* Corresponding author. Tel.: +86 411 84707636; fax: +86 411 84709284.
E-mail address: wangl@dlut.edu.cn (L. Wang).

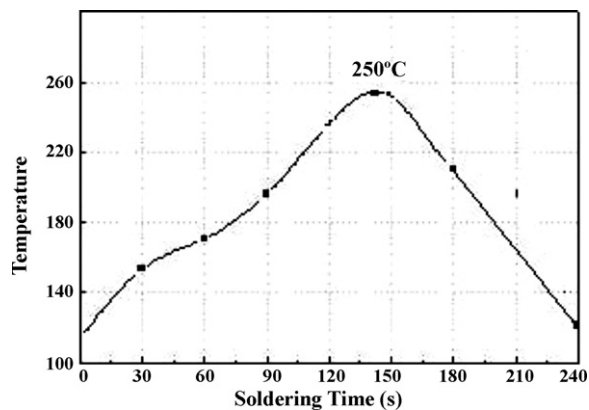


Fig. 1. Temperature profiles for a solder bump during reflow. The cooling rate is about 4 K s^{-1} .

in a 10 vol.% water solution of HNO_3 , followed by cleaning in ethanol and drying in air. Patches of solder paste, with a diameter of 5 mm and a height of 1 mm, were laid on the Cu substrates, put into the oven with the soldering profile shown in Fig. 1 and then cooled in air. The soldering temperatures were 250°C and 300°C .

The soldering durations were 30 s, 60 s, 120 s, 300 s, 600 s and 1800 s, respectively. In order to observe the morphologies of IMCs, the bulk solder was removed by deep etching in 10 vol.% HNO_3 dissolution with ultrasonic wave. The morphologies of the solder joints as well as the IMCs interface were studied using a scanning electron microscope (SEM). Energy dispersive spectroscopy (EDS) and X-ray diffraction (XRD) were also used to analyze the composition of selected area.

3. Results

3.1. The adsorption of Ag_3Sn particles

The three-dimensional structure of the interfacial $\eta\text{-Cu}_6\text{Sn}_5$ was observed by selectively etching the bulk solder. Fig. 2 shows the SEM top views of the IMCs on Sn–3Ag–0.5Cu/polycrystalline Cu interface soldered for different times at 250°C . It is clear that the scallop-shaped $\eta\text{-Cu}_6\text{Sn}_5$ grains with the size of $1.5\ \mu\text{m}$ were formed at the interface soldered for 30 s (Fig. 2A). Meanwhile some light-colored nano-particles which were estimated to be Ag_3Sn (shown in Fig. 3) with the size of 200 nm were found around the IMCs. With the increasing soldering time, the bigger Cu_6Sn_5 compounds incorporated the smaller ones sideward to form bigger scallop-shaped Cu_6Sn_5 compounds in a ripening process and the

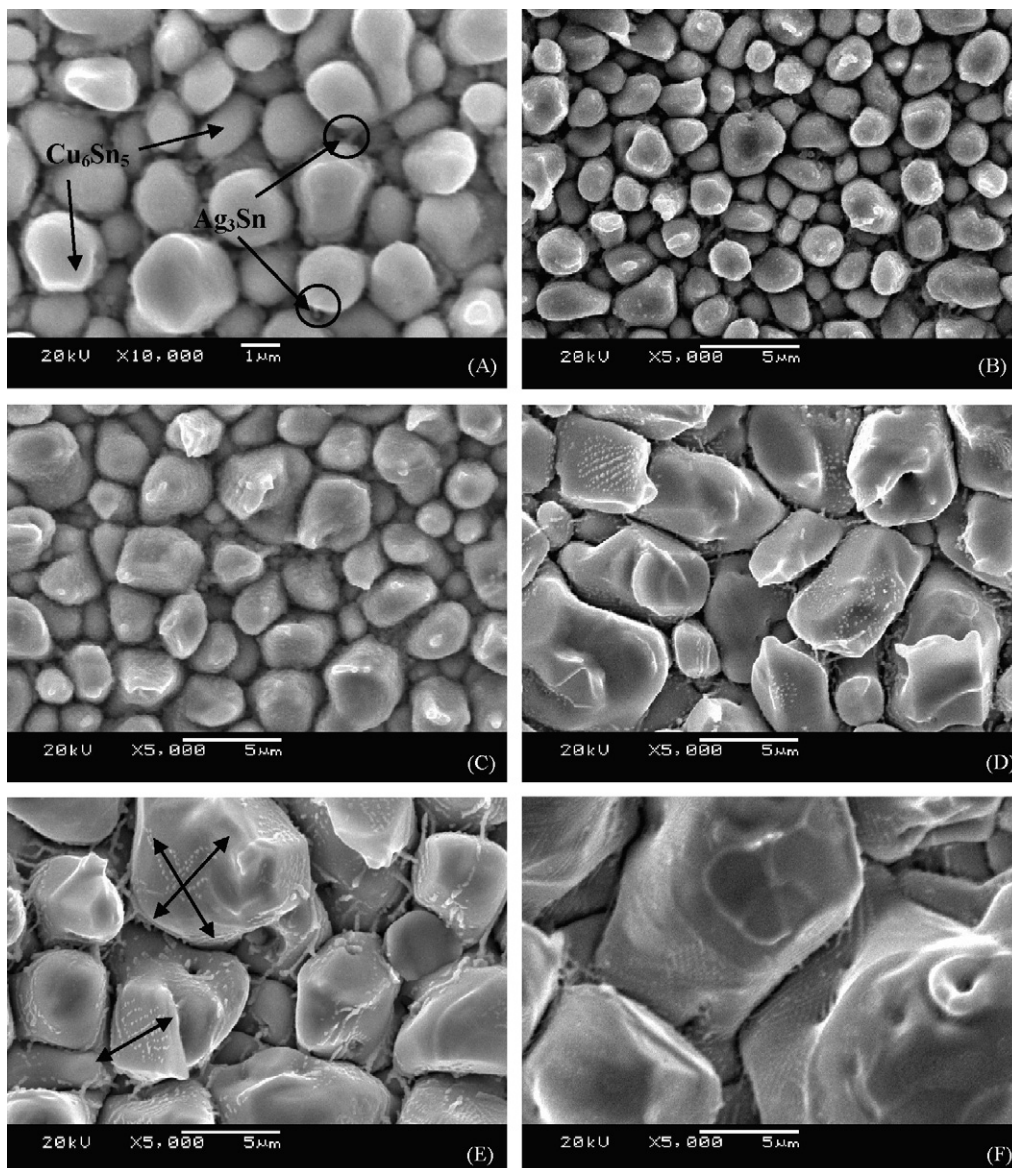


Fig. 2. The SEM images of the IMC of Sn–3Ag–0.5Cu/polycrystalline Cu soldering at 250°C : (A) 30 s, (B) 60 s, (C) 120 s, (D) 300 s, (E) 600 s and (F) 1800 s.

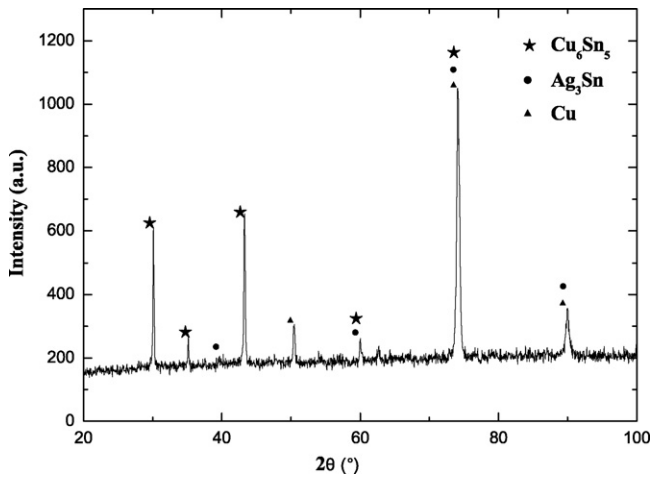


Fig. 3. XRD patterns of interfacial IMC at Sn-3Ag-0.5Cu/polycrystalline Cu joints reflowed at 250 °C for 30 s.

morphologies of Cu_6Sn_5 compounds became flat. Compared with the samples soldered for 30 s, it can be seen that more Ag_3Sn particles adsorbed on the surface of IMCs soldered for 5 min. However, the Ag_3Sn phases did not have obvious changes in size with the increasing soldering time.

Fig. 4 shows the morphology of IMCs on Sn-3Ag-0.5Cu/polycrystalline Cu interface soldered at 300 °C for different times. From SEM and XRD analysis, the compositions of IMC grains soldering for different times were the same while the IMCs morphologies changed from facet to stick-shape. The elongated stick-shaped IMCs were found at the interface and the length of these IMCs was about 30 μm soldered for 30 s (Fig. 4A). It is well known that in the liquid tin–solid copper system, more complex growth mechanisms govern the formation and morphological evolution of the interfacial layers, giving a scalloped interface between the η phase and liquid tin. However, Gagliano and Fine [17] had reported that Cu_6Sn_5 whiskers were also observed in the solidified tin and noted to emanate from the top of the η scallops. The same phenomenon was also observed in the present work. After soldering for 5 min, the longer Cu_6Sn_5 column broke off or dissolved into the matrix and Cu_6Sn_5 grains tended to form the scallop-type morphologies.

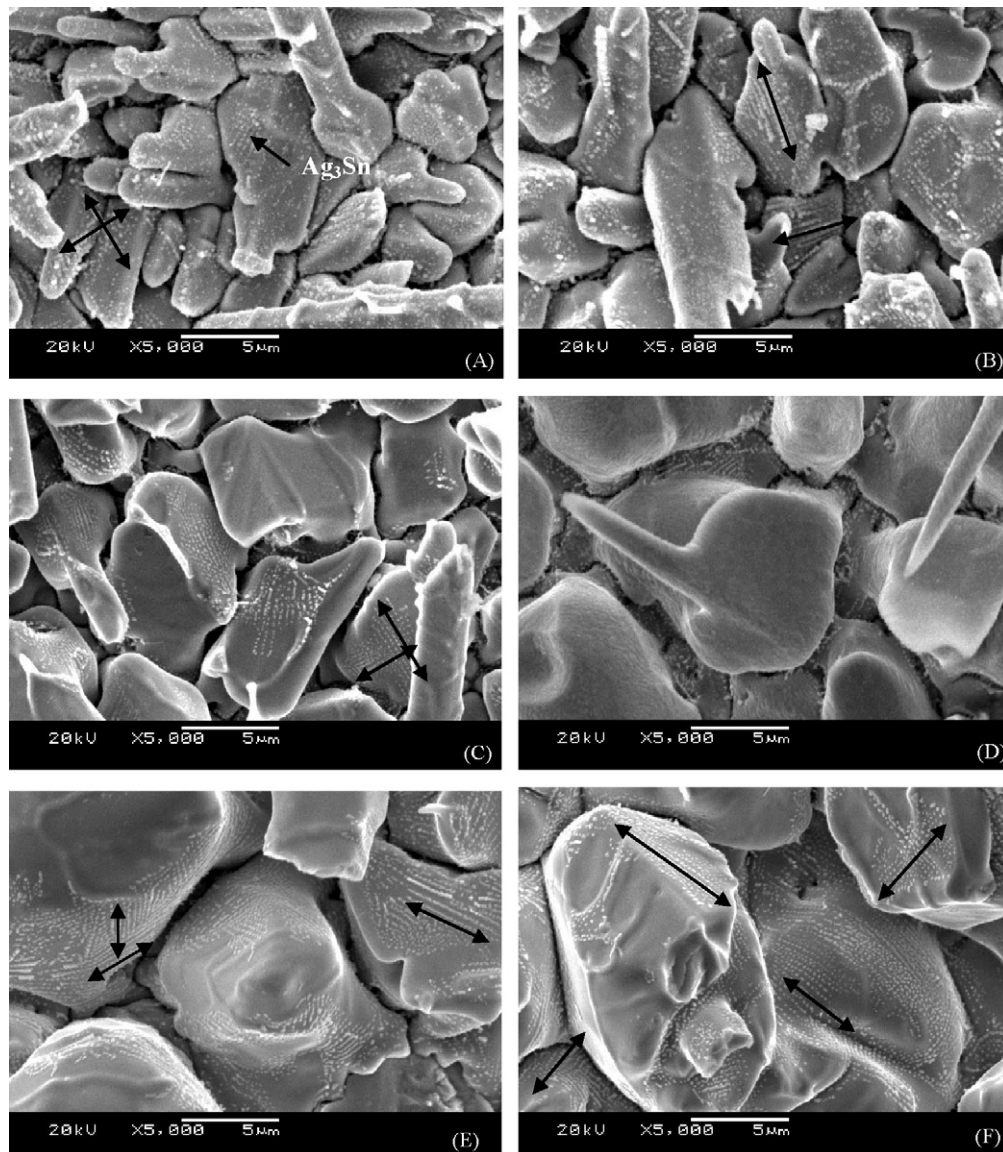


Fig. 4. The SEM images of the IMC of Sn-3Ag-0.5Cu/polycrystalline Cu soldering at 300 °C: (A) 30 s, (B) 60 s, (C) 120 s, (D) 300 s, (E) 600 s and (F) 1800 s.

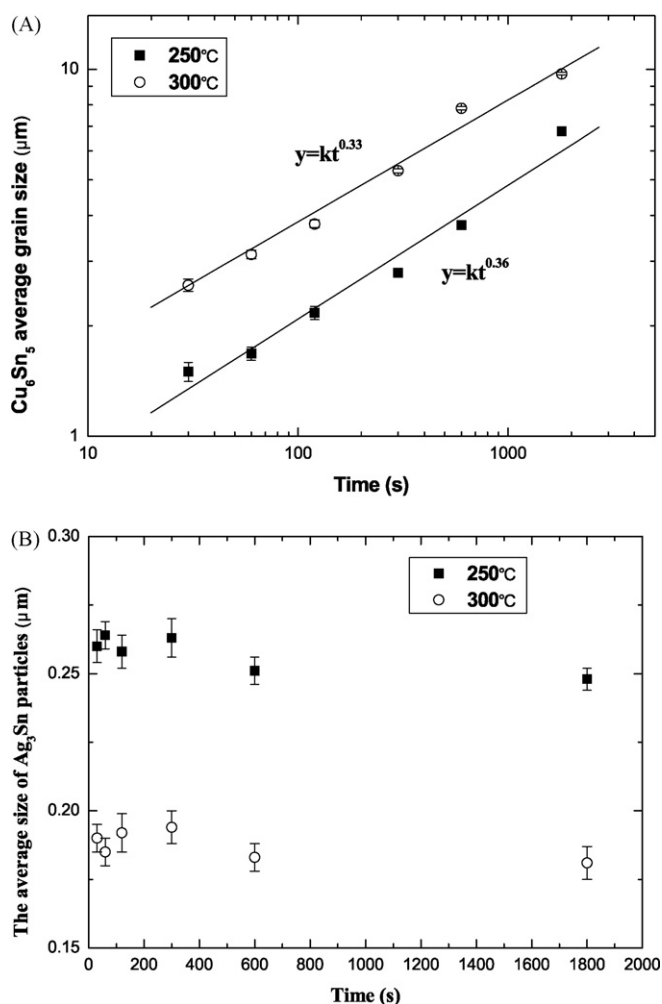


Fig. 5. Data plots of average diameter vs. time in reaction at different temperatures: (A) Cu_6Sn_5 grains and (B) Ag_3Sn nano-particles.

Compared with that soldering at 250 °C, the size of Ag_3Sn particles soldering at 300 °C was smaller and the number was increased. The average sizes of Cu_6Sn_5 and Ag_3Sn compounds were shown in Fig. 5.

3.2. The effect of cooling rate on the size of Ag_3Sn nano-particles

From the experiment, it is obvious that when soldering for different times at a fixed temperature, increasing soldering time had only little effect on the size of the Ag_3Sn particles. In order to verify this conclusion, the different cooling rate was used in subsequent experiment. The soldering process of Sn–Ag–Cu alloy had been reported in Section 2 except that the solder was cooled in water after melting in oven. The primary cooling rate was about 30 °C/s, and the melting temperature profile is the same as that shown in Fig. 1. Fig. 6 shows the top images of Cu_6Sn_5 grains and Ag_3Sn particles adsorption at a rapid cooling rate. The size of Ag_3Sn particles was smaller than that cooled in air. It indicated that the formation of Ag_3Sn particles took place in the solidification process. It is well known that the undercooling increased with the cooling rate. As a result, a high nucleation rate was obtained from a high undercooling rate.

3.3. The adsorption of Ag_3Sn nano-particles on (001) Cu single crystal

Zou et al. [18] had found that the regular prism-type Cu_6Sn_5 grains formed on (001) Cu single crystals were elongated either

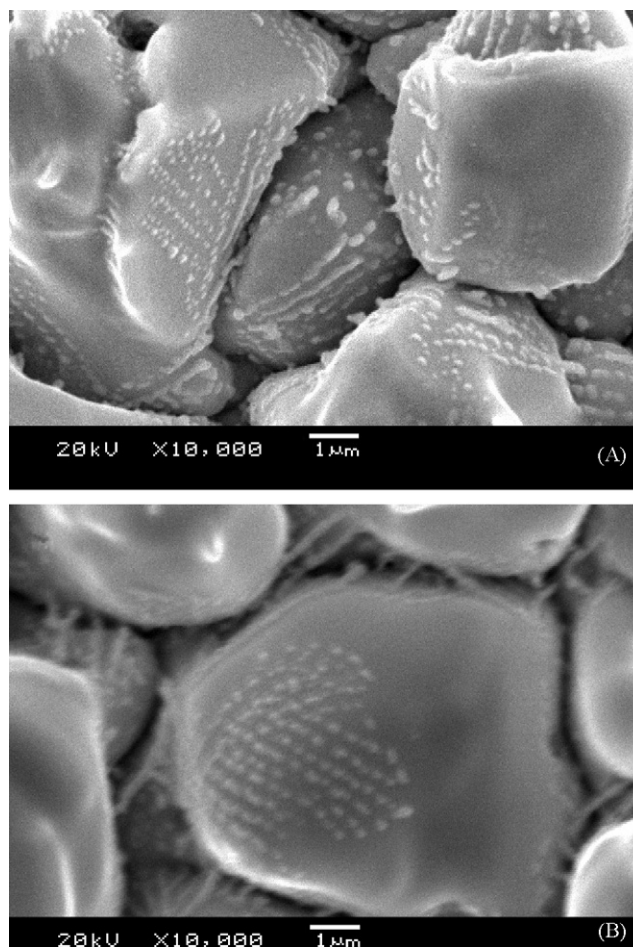


Fig. 6. The morphology of IMC cooling at different rate: (A) cooled in air and (B) cooled in water.

along two perpendicular directions. In order to make sure whether there was a relationship between the orientation of Cu_6Sn_5 compounds and the arrangement of Ag_3Sn nano-particles, the (001) Cu single crystal was used as substrate. In the previous literature [19], Cui had found that the scallop-type Cu_6Sn_5 formed on (001) single crystal Cu at 250 °C, but the prism-type Cu_6Sn_5 generated at 300 °C. So the temperature in the present work was 300 °C. The SEM top view images of Cu_6Sn_5 compounds soldering at 300 °C for 5 min were shown in Fig. 7. It is very interesting to see that the Ag_3Sn particles are arranged in a line. The plane of area 4 was parallel to that of areas 1 and 2. The arrangement of Ag_3Sn nano-particles in area 2 was elongated along two perpendicular directions, but it was not parallel to the arrangement in area 1. The arrangement directions of Ag_3Sn nano-particles in area 4 were parallel to that in area 5. It indicated that the orientation of Cu_6Sn_5 surface had no effect on the arrangement of Ag_3Sn nano-particles. From the above experiments, it became obvious that the arrangement directions of Ag_3Sn nano-particles were not controlled by the orientation of Cu_6Sn_5 surface. The ordered structures of Ag_3Sn had been formed in liquid solder and the formation mechanism of orientation was controlled by the growth orientation of Ag_3Sn compounds in solder matrix.

4. Discussion

In the Sn–3Ag–0.5Cu solder, precipitate Ag_3Sn phase existed. Bian et al. [20] had investigated the liquid structure of Cu–Al, Al–Ni, etc. and reported that if IMC formed in the alloys, there would exist

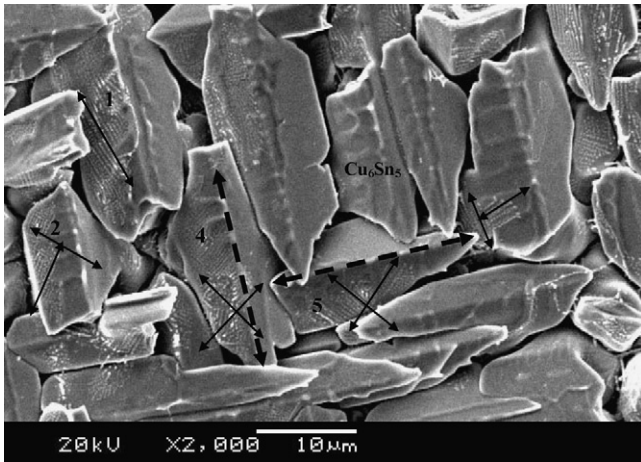


Fig. 7. SEM top view images of Cu_6Sn_5 compounds and Ag_3Sn nano-particles on (001) Cu single crystal substrate.

not only short-range order (SRO) structure but also medium-range order (MRO) in the liquid metal under certain condition. Because the higher affinity between Sn and Ag as well as the lower temperature there maybe not only SRO Ag_3Sn groups but also MRO Ag_3Sn groups in the liquid solder, Ag atoms first react with Sn to form Ag_3Sn phase in liquid solder. During solidification process, the Ag_3Sn phase precipitate near the IMCs and are likely to be “captured” by the IMCs.

The interface free energy of crystal G can be given by:

$$G = \sigma A \quad (1)$$

where σ is the surface energy and equals to the surface tension in numerical value; A is the surface area of the grain or the plane. Due to the same surface tensions between Cu_6Sn_5 grains and liquid solder for these joints, based on Eq. (1), the larger Cu_6Sn_5 grains have higher interface free energies. So it is easy to absorb the Ag_3Sn nano-particles on the large and smooth Cu_6Sn_5 grains. The adsorption will decrease the surface energy of the Cu_6Sn_5 compounds and retard the growth of the whole IMC layer [14].

The Gibbs absorption equation is expressed as [21]:

$$\Gamma = -\frac{x}{RT} \left(\frac{d\sigma}{dx} \right)_T \quad (2)$$

where Γ is the differential concentration at unit interface between the solute at surface and that inside the adjacent solution; x is the gram-atom fraction; R is the general gas constant; T is the absolute temperature and $(d\sigma/dx)_T$ gives the change of surface tension with the concentration at a given temperature. If the solute reduces the surface energy of the interface, its concentration at the interface will be much higher than that inside the solution. In other words, adsorption at the interface is likely to occur at this condition. It is well known that the larger the surface tension is, the faster the plane grow and the more the amount of surface-active materials adsorb [22]. The Ag_3Sn nano-particles play the role of surface energy reducer for the growth of interfacial Cu_6Sn_5 grains during the solidification.

The formation of Ag_3Sn nano-particles and the theory of surface-active material adsorption are used to explain the effect of the surface energy decreasing of IMCs [14]. Although it is quite difficult to calculate the interfacial energy, it is obvious that the adsorption will decrease the surface energy of the compounds. Furthermore, it is no doubt that the existence of them would restrain the growth of the whole IMCs layer during aging process.

The morphologies of the Cu_6Sn_5 IMCs at different soldering temperature are distinct from each other. The interfacial reactions forming IMC layers are governed by release of free energy.

But in order to have the largest negative free energy change in a short time, the rate of free energy change becomes more important and the high rate of free energy change is favorable [23]. Tu et al. has regarded that which reaction path can give the largest rate of free energy change may depend on the morphology and microstructure of the product phase. For example, the scallop-type IMC had a high growth rate at the interface of Sn–Ag–Cu/Cu [24]. As shown in Figs. 2 and 4, the morphologies of the Cu_6Sn_5 change obviously.

The average sizes of the Ag_3Sn particles on the surface of the η - Cu_6Sn_5 were the same when soldering from 30 s to 1800 s at a certain temperature. The effects of soldering time and temperature on the average sizes of Ag_3Sn particles are quite intricate. The change of average size and number of the Ag_3Sn nano-particles is caused by a number of factors. First, it has been found that the presence and the disappearance of the MRO structures in molten metals were a function of temperature and was corresponded to the tendency towards chemical compound formation [25]. If IMCs were formed in the alloy, the distribution of the atoms was not random in microstructure in liquid state. The IMC structure in liquid state can be kept in the solid state if the liquid temperature has not exceeded the melting temperature too much. When soldering at 250 °C, the soldering temperature is only 33 °C above the melting temperature and the affinity between Sn and Ag is higher. The ordered groups are more dominant. This explains why soldering at a fixed temperature, the size of adsorbed Ag_3Sn particles are the same. However, when the soldering temperature is 300 °C, which is 83 °C above the melting temperature, Ag_3Sn structure in liquid state is liberated and ordered Ag_3Sn groups are less prevalent. Thus, the sizes of adsorbed Ag_3Sn particles are smaller than those at 250 °C.

Secondly, the size of the Cu_6Sn_5 IMCs plays an important role in adsorbing the Ag_3Sn particles. The bigger the Cu_6Sn_5 IMC, the larger the interfacial energy. So in order to decrease the surface energy of the compound, more Ag_3Sn particles are to be adsorbed on the surface. Based on above analysis, the number of Ag_3Sn nano-particles increases with increasing soldering time. Due to the cooling rate for the same substrate is nearly the same with the different soldering time, the Ag_3Sn phase will have the same size. This reason explains why the soldering time had little effect on the Ag_3Sn particle size.

From Fig. 2(E) and (F) and Fig. 4(E) and (F), it can be seen that the Ag_3Sn particles arranged in lines in the same plane and the arrangement of Ag_3Sn particles ordered two perpendicular orientations. This phenomenon is difficult to explain. Zou et al. [26] has reported the regular Ag_3Sn compounds with parallel edges formed between molten Sn and (001) Ag single crystals went along two perpendicular directions. Moreover the three-dimensional morphology of Ag_3Sn compounds in solder matrix still has the same phenomenon [5]. In the present study, the arrangement of Ag_3Sn nano-particles may have the relationship with the Ag_3Sn compounds in solder matrix. They gather with the same growth orientation of Ag_3Sn compounds in liquid solder and are “captured” by IMCs during cooling process.

5. Conclusions

The reactions between Sn–3Ag–0.5Cu/polycrystalline or (001) single crystal Cu substrate at 250 °C and 300 °C were investigated in the present study. Adsorption of Ag_3Sn particles was found on the Cu_6Sn_5 IMCs surface during the reflowing process. The results showed that the morphologies of the Cu_6Sn_5 IMCs were changed with different soldering temperature and time. The sizes of adsorbed Ag_3Sn nano-particles were almost the same with the different soldering durations, but the particles were smaller at high temperature (300 °C) than those at low temperature (250 °C), and they were also smaller when specimen were cooled in water com-

pared to those cooled in air. The Ag_3Sn particles are arranged in line in the same plane and the arrangements of Ag_3Sn lines order two perpendicular orientations, but there are no relationship with the Cu_6Sn_5 surface orientation. The arrangement of Ag_3Sn particles may be affected by the growth orientation of Ag_3Sn compounds in liquid solder and the particles were “captured” by IMCs during cooling process.

Acknowledgements

This work is supported by National Key Technologies R&D Program (2006BAE03B02-2), NSFC key program (U0734006), and Key Laboratory Program in Liaoning Province (20060133). The authors would like to thank Prof. Lawrence Wu at City University of Hong Kong for his cooperation in this study.

References

- [1] F. Wang, M. O’Keefe, B. Brinkmeyer, *J. Alloys Compd.* 477 (2009) 267–273.
- [2] U. Büyüç, N. Marassh, *J. Alloys Compd.* 485 (2009) 264–269.
- [3] C.L. Wei, C.R. Kao, Proceedings of the 4th International Symposium on Electronic Materials and Packaging Conference, IEEE Press, Taiwan, China, 2002, pp. 330–334.
- [4] C.Y. Lin, J.H. Chou, Y.G. Lee, U.S. Monhanty, *J. Alloys Compd.* 470 (2009) 328–331.
- [5] H.T. Lee, Y.F. Chen, T.F. Hong, K.T. Shih, 2009 International Conference on Electronic Packaging Technology & High Density Packaging, 2009, p. 646.
- [6] K.S. Kim, S.H. Huh, K. Suganuma, *J. Alloys Compd.* 352 (2003) 226–236.
- [7] H.W. Tseng, C.Y. Liu, *Mater. Lett.* 62 (2008) 3887–3889.
- [8] F.L. Zhu, H.H. Zhang, R.F. Guan, S. Liu, *J. Alloys Compd.* 438 (2007) 100–105.
- [9] K.S. Kim, S.H. Huh, K. Suganuma, *Mater. Sci. Eng. A: Struct.* 333 (2002) 106–114.
- [10] D.R. Frear, J.W. Jang, J.K. Lin, C. Zhang, *JOM* 53 (2001) 28–33.
- [11] J. Zhao, Y. Miyashita, Y. Mutoh, *Int. J. Fatigue* 23 (2001) 723–731.
- [12] K. Zeng, K.N. Tu, *Mater. Sci. Eng. R* 38 (2002) 55–105.
- [13] F. Guo, S. Choi, K.N. Subramanian, T.R. Bieler, J.P. Lucas, A. Achari, M. Paruchuri, *Mater. Sci. Eng. A: Struct.* 351 (2003) 190–199.
- [14] D.Q. Yu, L. Wang, C.M.L. Wu, C.M.T. Law, *J. Alloys Compd.* 389 (2005) 153–158.
- [15] C.M.L. Wu, M.L. Huang, *IEEE Trans. Adv. Packag.* 28 (2005) 128–133.
- [16] L.H. Qi, J.H. Huang, X.K. Zhao, H. Zhang, *J. Alloys Compd.* 469 (2009) 102–107.
- [17] R.A. Gagliano, M.E. Fine, *JOM* 53 (2001) 33–38.
- [18] H.F. Zou, H.J. Yang, Z.F. Zhang, *Acta Mater.* 56 (2008) 2649–2662.
- [19] Y.P. Cui, M.L. Huang, 2009 International Conference on Electronic Packaging Technology & High Density Packaging, 2009, p. 593.
- [20] X.F. Bian, P.X. Min, X.B. Qin, M.H. Jiang, *Sci. China (Series E)* 32 (2002) 145–151.
- [21] J. Shen, Y.C. Chen, *J. Alloys Compd.* 477 (2009) 909–914.
- [22] J. Wang, L.G. Zhang, H.S. Liu, L.B. Liu, Z.P. Jin, *J. Alloys Compd.* 455 (2008) 159–163.
- [23] C.M.L. Wu, D.Q. Yu, C.M.T. Law, *Mater. Sci. Eng. R* 44 (2004) 1–44.
- [24] K.N. Tu, K. Zeng, *Mater. Sci. Eng. R* 34 (2001) 1–58.
- [25] I.E. Anderson, B.A. Cook, J. Harringa, R.L. Terpatra, *J. Electron. Mater.* 31 (2002) 1166–1174.
- [26] H.F. Zou, H.J. Yang, J. Tan, Z.F. Zhang, *J. Mater. Res.* 24 (2009) 2141–2144.